

Contrast-enhanced magnetic resonance imaging assessment of scar size in patients with chronic myocardial infarction

Oronzo Catalano, Serena Antonaci, Guido Moro*, Giorgio Cannizzaro**, Renato Mingrone, Cristina Opasich, Mauro Frascaroli*, Felice Rognone*, Maurizia Baldi*, Roberto Tramarin

Division of Cardiology, *Radiology Service, **Nuclear Imaging Service, IRCCS S. Maugeri Foundation, Pavia, Italy

Key words:

Echocardiography; Magnetic resonance imaging; Myocardial infarction; Single-photon emission computed tomography.

Background. In the assessment of myocardial infarction (MI) mass, contrast-enhanced magnetic resonance imaging (CE-MRI) is comparable to single-photon emission computed tomography (SPECT). The aim of the present study was to determine whether the MI area, as assessed at CE-MRI and SPECT, is comparable to mass evaluation. We also compared CE-MRI and SPECT estimates of the MI area with functional evaluations made at echocardiography and kinetic MRI (cine-MRI).

Methods. We used a 1.0 Tesla MRI scanner and an inversion-recovery turboFLASH sequence, a tomographic gamma-camera and second-harmonic ultrasound systems. Two blinded operators assessed the extent of scarring, expressed as a percentage of the whole left ventricle (LV), using a 16-segment model. We studied 55 consecutive patients with a clinically stable healed MI (50 Q wave, 5 non-Q wave).

Results. The scar mass was $19 \pm 23\%$ of the LV at CE-MRI and $21 \pm 25\%$ at SPECT; the scar area was $29 \pm 23\%$ of the LV at CE-MRI, $41 \pm 28\%$ at SPECT, $29 \pm 31\%$ at cine-MRI, and $32 \pm 29\%$ at echocardiography. The Bland-Altman bias between CE-MRI and SPECT mass estimations was -2% of the LV with a $\pm 23\%$ limit of agreement (LOA), while the bias between the area assessments was -12% with a $\pm 42\%$ LOA. Bias between CE-MRI and functional evaluation by cine-MRI and echocardiography was 0% with a $\pm 39\%$ LOA and -3% with a $\pm 36\%$ LOA respectively. Comparing SPECT with cine-MRI and echocardiography the bias was 12% with a $\pm 52\%$ LOA and 9% with a $\pm 56\%$ LOA respectively.

Conclusions. CE-MRI has proved to be comparable to SPECT in the assessment of the healed MI mass. Conversely, a high systematic error (high bias and LOA) renders CE-MRI and SPECT assessments of the MI area incomparable. Similarly (high bias and/or LOA) CE-MRI and SPECT estimations of the MI area cannot be compared with functional evaluation by echocardiography or cine-MRI.

(Ital Heart J 2005; 6 (2): 133-137)

© 2005 CEPI Srl

Received July 14, 2004;
revision received
December 14, 2004;
accepted December 16,
2004.

Address:

Dr. Oronzo Catalano

Divisione di Cardiologia
IRCCS Fondazione
S. Maugeri
Via Ferrata, 4
27100 Pavia
E-mail: ocatalano@fsm.it

Introduction

The infarct size is a critical parameter in the prediction of left ventricular remodeling and congestive heart failure. In clinical practice it is usually assessed at transthoracic echocardiography and single-photon emission computed tomography (SPECT), which respectively detect kinetic abnormalities and perfusion defects due to necrotic myocardium or scarring. The extent of a myocardial infarction (MI) may also be assessed at magnetic resonance imaging (MRI), which directly visualizes necrotic myocardium and scarring using gadolinium-based contrast agents¹⁻⁶. Interestingly, MRI is an imaging technique which does not expose the patient to ionizing radiations and which yields highly defined images whose quality is very good in patients who are able to tolerate short periods of apnea (10-15 s). Moreover, the image quality of

MRI is not modified by the patient's characteristics such as a suboptimal acoustic window or high body mass index. The MI size as evaluated at contrast-enhanced MRI (CE-MRI) seems to have a reproducibility at least comparable to that of SPECT⁷. Furthermore, infarct mass estimations by CE-MRI and SPECT have been shown to be very similar⁷. The aim of the present study was to determine whether the MI area, as assessed at CE-MRI and SPECT, is comparable to mass evaluation. In addition, the MI area estimated at CE-MRI and SPECT were compared with the extent of wall motion abnormalities as assessed at echocardiography and kinetic MRI (cine-MRI).

Methods

The study was approved by the Institutional Review Board. Cardiac MRI was

performed, after informed consent, in a group of patients referred to our Division for clinically stable chronic MI. Routine evaluation of these patients includes SPECT and echocardiographic studies. A standard 16-segment partition of the left ventricle (LV) was used for all imaging techniques (Fig. 1). A semiquantitative assessment of the segmental contractility, delayed enhancement and perfusion status (Table I) was obtained by consensus of two skilled operators for each technique, blinded with respect to the results of the other tests. For all evaluations, the MI area was calculated as the percent of the LV showing any morphologic, perfusion or kinetic abnormalities. For CE-MRI and SPECT an estimation of the MI mass was obtained by assuming a segmental score to reflect the progressive transmural extent of the scar. This is true for MRI and may also be an acceptable approximation for SPECT.

Magnetic resonance imaging. We used a 1.0 Tesla scanner (Magnetom Harmony, Siemens) with a 20 mT gradient and a phased-array coil. Breath-hold ECG-gated cine gradient-echo sequences (repetition time 45 ms,

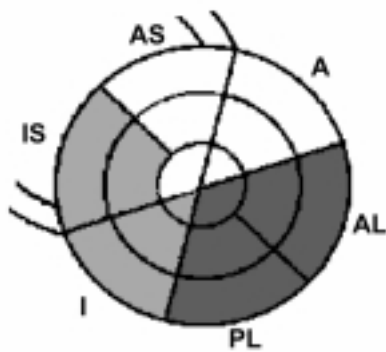


Figure 1. Sixteen-segment model of the left ventricle used to evaluate contrast-enhanced magnetic resonance imaging, single-photon emission computed tomography and echocardiographic images. The left anterior descending coronary artery territory includes 6 segments (white segments): the anterior septum (AS), anterior wall (A), septal apex, and anterior apex. The circumflex coronary artery territory includes 5 segments (dark grey segments): the antero-lateral wall (AL), postero-lateral wall (PL), and lateral apex. The right coronary artery territory includes 5 segments (light grey): the inferior wall (I), inferior septum (IS), and inferior apex.

echo time 6.1 ms, flip angle 20°, matrix 126 × 256, field of view 350 mm) for wall motion analysis, and inversion-recovery turboFLASH sequences (echo time 2.6 ms, flip angle 8°, inversion time 260-360 ms, matrix 96 × 256, field of view 400 mm) for scar detection 5 min after the intravenous injection of 0.15 mmol/kg gadopentetate-dimeglumine or gadomenate-dimeglumine (Magnevist; Schering; Multihance, Bracco), were taken. Full ventricular coverage was obtained with 10 mm thick multiple (usually 8) short-axis views. Moving from the base to the apex of the LV, slices 1-3 were considered as covering the basal segment, slices 4-6 the mid segment, and slices 7-8 the apex of the LV. The transmural extent of delayed enhancement was scored using a 4-point scale¹ (Table I). The score of each of the 16 segments was then calculated from the average of the three values (two values for the apical ones). The acquisition and evaluation of the images lasted approximately 30 min.

Single-photon emission computed tomography. SPECT study was performed 45-60 min after the administration of 740 MBq tetrofosmin at rest, equivalent to an effective dose of 5.36 mSv for a 70 kg patient. A large field of view tomographic gamma-camera (Apex-SP6, Elscint) equipped with a high resolution collimator and a 20% window centered on the 140 KeV photopeak of technetium-99m, was used. Images were reconstructed by filtered back-projection with no attenuation or scatter correction. Tracer activity was normalized on the maximal left ventricular activity. Color encoded short-axis images were used to build a bull's-eye display of activity. A 16-segment model of the LV (Fig. 2) was superimposed on the polar plots and the tracer activity was scored using a 4-point system^{8,9} (Table I). Horizontal long-axis, vertical long-axis and short-axis slices were simultaneously available and used to confirm the polar map assessments.

Echocardiography. The regional left ventricular systolic function was evaluated by assessing wall thickening and endocardial excursion (radial shortening)^{10,11} at

Table I. Semiquantitative assessment of the segmental contractility, delayed enhancement and perfusion.

		Segmental score			
	Applied to	0	1	2	3
Wall thickening/ radial shortening	Cine-MRI and echo	Normal	Hypokinesia	Akinesia	Dyskinesia or reduced thickness*
Delayed enhancement (% of wall thickness)	CE-MRI	Absent	< 25%	25-75%	> 75%
Perfusion	SPECT	Normal	Mildly reduced	Moderately reduced	Severely reduced or absent

CE-MRI = contrast-enhanced magnetic resonance imaging; echo = transthoracic echocardiography; SPECT = single-photon emission computed tomography. * < 5 mm.

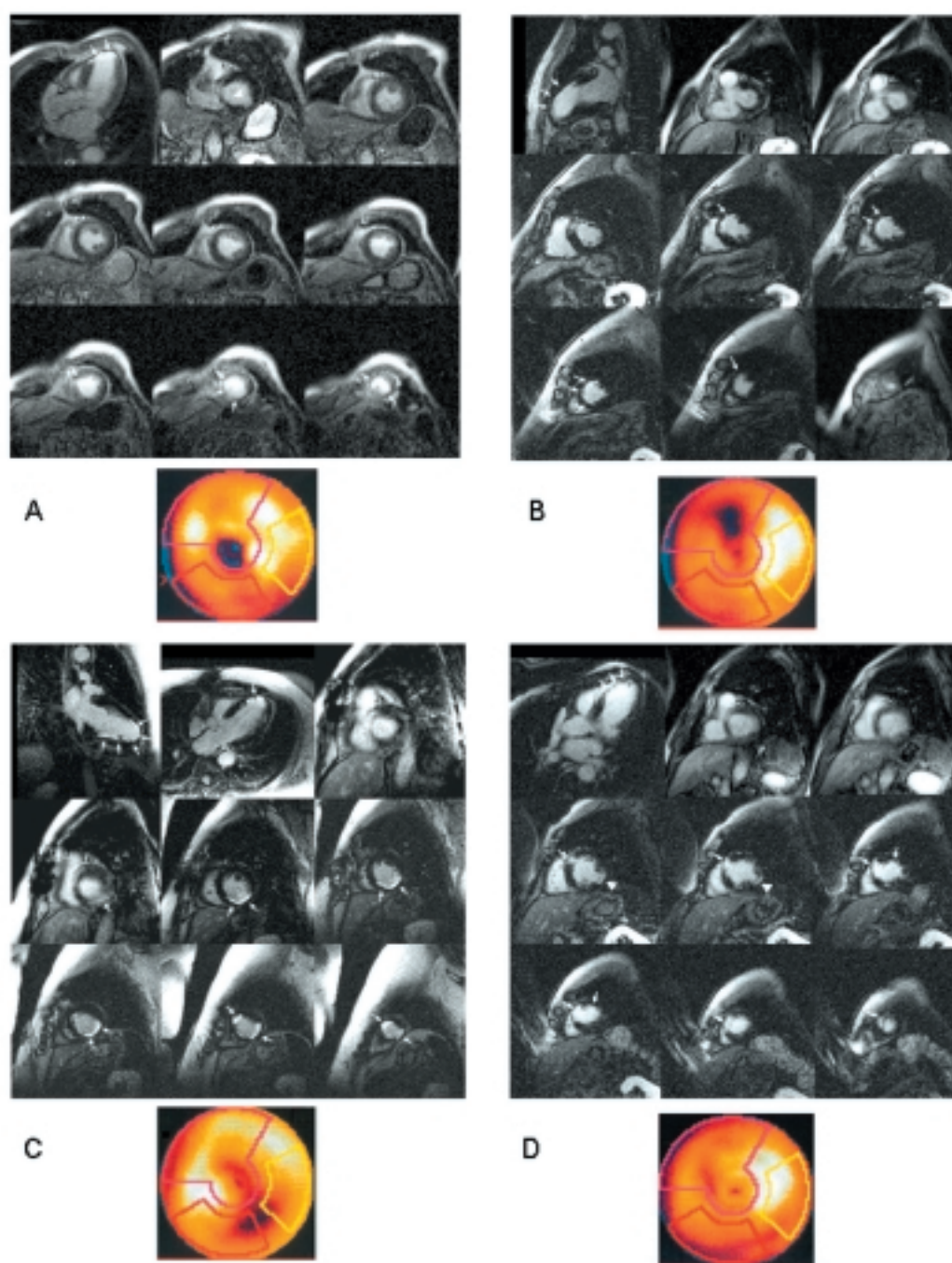


Figure 2. Examples of myocardial infarctions assessed as delayed enhancement at magnetic resonance imaging and as rest perfusion defect at single-photon emission computed tomography. In each panel magnetic resonance imaging long-axis views (more appropriate ones) and contiguous multiple short-axis views of the contrast-enhanced magnetic resonance imaging study (upper part) and color encoded bull's-eye display of single-photon emission computed tomography rest perfusion assessment (lower part) are shown. Panel A: small subendocardial scarring in the basal segment of the postero-lateral wall (arrow tip) and medium size transmural scarring involving the septal-apical and inferior-apical segments detected at contrast-enhanced magnetic resonance imaging (arrows) as well as at single-photon emission computed tomography. Panel B: medium size subendocardial scarring of the mid-anterior wall detected at contrast-enhanced magnetic resonance imaging (arrows) as well as at single-photon emission computed tomography. Panel C: large subendocardial scarring involving the mid-distal segment of the infero-lateral wall and the apical segments of the septum and lateral wall as seen at contrast-enhanced magnetic resonance imaging (arrows) as well as at single-photon emission computed tomography. Panel D: small subendocardial scarring in the mid-segment of the postero-lateral wall, as seen at contrast-enhanced magnetic resonance imaging (arrow tip) but not at single-photon emission computed tomography, and medium size scarring involving the mid-distal segment of the anterior septum as seen at contrast-enhanced magnetic resonance imaging (arrows) and at single-photon emission computed tomography. Mild perfusion defect in the basal segment of the inferior and infero-lateral walls at single-photon emission computed tomography without the related delayed enhancement at magnetic resonance imaging, suggesting attenuation.

second harmonic two-dimensional echocardiography (Sequoia, Acuson; Sonos 5500, Hewlett Packard). A multisection approach was used by assessing the para-

sternal short- and long-axis views and the 3-, 4-, and 5-chamber apical views. The regional contractility was scored on a 4-point scale (Table I).

Statistical analysis. Discrete variables are expressed as counts or percentages. Continuous variables are expressed as means \pm SD. The Bland-Altman method was used for intertechnique comparison of the infarct size¹². Statistical significance was assessed using the Wilcoxon signed-rank test. A *p* value < 0.05 was considered as statistically significant.

Results

Fifty-seven consecutive patients met the enrolment criteria of the study. Two (4%) were excluded because they were claustrophobic and 55 were evaluated: 50 had a history of Q wave MI and 5 of non-Q wave MI. MRI was performed within 7 ± 8 and 8 ± 9 days of echocardiography and SPECT respectively. In all patients the MRI and SPECT image quality was judged to be adequate. The echo image quality was considered insufficient in 5 patients, who however were not excluded from the analysis as an approximate judgment on the segmental contractility was all the same provided by the echocardiographers. The clinical features of the patient population are reported in table II.

The MI mass estimation was $19 \pm 23\%$ of the LV as assessed by means of delayed enhancement at CE-MRI and $21 \pm 25\%$ as assessed by means of perfusion defect at SPECT (Wilcoxon signed-rank test, *p* = NS). Therefore, the average difference (Bland-Altman bias) was -2% of the LV with a $\pm 23\%$ limit of agreement (LOA).

The MI area was $29 \pm 23\%$ of the LV at CE-MRI and $41 \pm 28\%$ at SPECT (*p* = 0.000). The average difference was -12% of the LV with a $\pm 42\%$ LOA. The MI area assessed as the extent of kinetic abnormalities was $29 \pm 31\%$ at cine-MRI and $32 \pm 29\%$ at echocardiography. The average differences between the functional evaluation at cine-MRI and echocardiography and the delayed enhancement estimation at CE-MRI were 0% and -3% of the LV (*p* = NS for both) with a $\pm 39\%$ and $\pm 36\%$ LOA respectively. The corresponding biases with the area of perfusion defect at SPECT were 12 and 9% (*p* = 0.003 and *p* = 0.022) with a $\pm 52\%$ and $\pm 56\%$ LOA respectively.

Table II. Clinical features of the study population.

Sex (M/F)	43/12
Age (years)	65 ± 9
Myocardial infarction site	
Anterior	24
Inferior/lateral	26
Non-Q	5
LVEF (%)	
≤ 30	8
31-40	7
41-50	12
> 50	28

LVEF = left ventricular ejection fraction.

Discussion

Our study confirms that assessments of MI mass at CE-MRI and SPECT are comparable. The Bland-Altman bias and LOA we obtained (-2% and $\pm 23\%$ of the LV) are very similar to the results reported by Mahrholdt et al.⁷ (-0.5% and $\pm 19.2\%$).

Although scarring is detected directly at CE-MRI through a morphologic evaluation and indirectly at SPECT through the resulting perfusion abnormalities, assessment of MI mass seems to be useful for comparing these two imaging techniques.

On the contrary, we found the estimations of the MI area at CE-MRI to be significantly lower than those obtained at SPECT (average bias -12% of the LV). An overestimation of the radial extent of scarring at SPECT, due to its low spatial resolution, may partly explain this difference. Moreover, SPECT may misleadingly identify areas of the LV showing the attenuation phenomenon as scar segments. This is especially true in case of obesity, rest ischemia or left bundle branch block, conditions which increase the incidence of artifacts. These conditions might contribute to an overestimation of the MI area at SPECT. Assessment of MI mass implied weighting the contribution of each segment by the degree of involvement (segmental score). As the reductions in radiotracer activity due to attenuation, a frequent pitfall in SPECT evaluation, but also to left bundle branch block are usually mild, the resulting inaccuracy is probably less significant for mass assessment.

The area of perfusion abnormalities at rest SPECT was found to be significantly larger than the extent of wall motion abnormalities at echocardiography and cine-MRI (average bias 12 and 9% of the LV, respectively). Besides confirming an overestimation of the MI area at SPECT, this finding discloses the intuitive idea that imaging techniques with very different information contents (perfusion, contractility) cannot be used indifferently to assess the MI size. On average, the area of delayed enhancement at CE-MRI was similar to the extent of wall motion abnormalities at echocardiography and cine-MRI (average bias 0 and -3% of the LV, respectively). Although the differences were not significant, the high LOA ($\pm 39\%$ and $\pm 36\%$ of the LV, respectively) renders this comparison biologically meaningless confirming that also morphologic and functional assessment of the MI cannot be easily compared. The high LOA may be due to the presence of delayed enhancements without wall motion abnormalities in case of very small scars and, on the other hand, to the occurrence of kinetic abnormalities without scar due to hibernation (stunned myocardium is expected to be infrequent in chronic MI).

Study limitations. We used a semiquantitative evaluation of MI mass and area consisting of a visual score for each of the 16 segments into which the LV was divided. Consequently we introduced some approximations

in MI assessment due to: segmentation, as the area of the various segments is not perfectly identical, heterogeneity of left ventricular wall thickness, for (asymmetric) hypertrophy or thinning of some transmural scarring and, above all, to the need of classifying a segment as being entirely scarred (with different transmural scores) when it was largely, but not completely, involved by MI (overestimation) and, conversely, as normal when it showed lesser involvement (underestimation). The results of our study are however very similar to those reported by Mahrholdt et al.⁷, who used a quantitative approach. This indirectly confirms the adequacy of the method we used.

In conclusion, CE-MRI proved to be comparable to SPECT for the assessment of the infarct mass in patients with a healed MI. The same cannot be said for the estimation of the scar area as a high systematic error was found when we compared CE-MRI to SPECT. Moreover, the extent of scarring as assessed at CE-MRI and SPECT cannot be compared with functional evaluation at echocardiography or cine-MRI.

Acknowledgments

Our study has been partly supported by the general research fund of the Italian “Ministero dell’Istruzione, dell’Università e della Ricerca”. We thank Mrs. De Conti for her precious collaboration in putting our study into practice.

References

1. Kim RJ, Fieno DS, Parrish TB, et al. Relationship of MRI delayed contrast enhancement to irreversible injury, infarct age, and contractile function. *Circulation* 1999; 100: 1992-2002.
2. Kim RJ, Wu E, Rafael A, et al. The use of contrast-enhanced magnetic resonance imaging to identify reversible myocardial dysfunction. *N Engl J Med* 2000; 343: 1488-90.
3. Simonetti OP, Kim RJ, Fieno DS, et al. An improved MR imaging technique for the visualization of myocardial infarction. *Radiology* 2001; 218: 215-23.
4. Wu E, Judd RM, Vargas JD, et al. Visualisation of presence, location, and transmural extent of healed Q-wave and non-Q-wave myocardial infarction. *Lancet* 2001; 357: 21-8.
5. Klein C, Nekolla SG, Bengel FM, et al. Assessment of myocardial viability with contrast-enhanced magnetic resonance imaging: comparison with positron emission tomography. *Circulation* 2002; 105: 162-7.
6. Wagner A, Mahrholdt H, Holly TA, et al. Contrast-enhanced MRI and routine single photon emission computed tomography (SPECT) perfusion imaging for detection of subendocardial myocardial infarcts: an imaging study. *Lancet* 2003; 361: 374-9.
7. Mahrholdt H, Wagner A, Holly TA, et al. Reproducibility of chronic infarct size measurement by contrast-enhanced magnetic resonance imaging. *Circulation* 2002; 106: 2322-7.
8. Danias PG, Ahlberg AW, Travin MI, et al. Visual assessment of left ventricular perfusion and function with electrocardiography-gated SPECT has high intraobserver and interobserver reproducibility among experienced nuclear cardiologists and cardiology trainees. *J Nucl Cardiol* 2002; 9: 263-70.
9. Danias PG, Ahlberg AW, Clark BA 3rd, et al. Combined assessment of myocardial perfusion and left ventricular function with exercise technetium-99m sestamibi gated single-photon emission computed tomography can differentiate between ischemic and nonischemic dilated cardiomyopathy. *Am J Cardiol* 1998; 82: 1253-8.
10. Aurigemma GP, Gaasch WH, Villegas B, Meyer TE. Non-invasive assessment of left ventricular mass, chamber volume, and contractile function. *Curr Probl Cardiol* 1995; 20: 361-440.
11. Lavine SJ, Salacata A. Visual quantitative estimation: semi-quantitative wall motion scoring and determination of ejection fraction. *Echocardiography* 2003; 20: 401-10.
12. Bland JM, Altman DG. Comparing methods of measurement: why plotting difference against standard method is misleading. *Lancet* 1995; 346: 1085-7.